

# The permanent thermal infrared network for the monitoring of hydrothermal activity at the Solfatara and Vesuvius volcanoes

G. Vilardo, G. Chiodini, V. Augusti, D. Granieri, S. Caliro,  
C. Minopoli, C. Terranova

*Istituto Nazionale di Geofisica e Vulcanologia, Osservatorio Vesuviano, Italy*

**Abstract:** In this paper we describe the activities carried out for the realization of an image surveillance systems, in the thermal infrared (TIR) wavelengths range, for the continuous long-term monitoring of the shallow thermal structure of the Solfatara (Campi Flegrei) and Vesuvius volcanoes. The system implementation was pursued by both acquiring and integrating all the technological instruments necessary to operate an instrumental system constituted by: a network of remote monitoring stations; a transmission system for the image data centralization; a control unit for both the remote stations control and the acquired data processing. The analysis of two-years long series of IR images collected at the Solfatara allowed us to evaluate, in the observation period, the main thermal features of the major fumarole field located in the SE inner slope of the Solfatara crater.

## INTRODUCTION

In recent years, following the hand-held thermal imaging cameras development, increasing use is being made of ground-based thermal IR measurements to map and investigate lava flow field structures, to estimate active lava flow parameters, to analyze the evolution of active eruption plumes (Pinkerton et al., 2002; Calvari and Pinkerton, 2004; Lautze et al., 2004; Calvari et al., 2005; Johnson et al., 2005; Harris et al., 2005; Vaughan et al., 2005; Lodato et al., 2006).

With respect to previous IR applications, most of which regarded the study of relatively quick processes associated to volcanic eruptions, our experiment was finalized to detect and quantify over long periods slow temperature changes of the shallow thermal structure of quiescent volcanoes. Any increase in the flux of fluid expelled by the volcanoes will be accompanied by an increase in the temperature of the rocks hosting the fumarolic vents or in the size of the fumarolically heated areas (Oppenheimer et al., 1993; Kaneko and Wooster,

1999). Moreover it is our opinion that also relatively slow variations in the amount of thermal energy flux can help to define the level of activity of the volcano and that possible major changes in surface temperature can mark the transition from a quiescent stage to an eruptive phase. For this reason our experiment was designed to monitor a significant portion of the Solfatara fumarolic field and the inner slope of the Vesuvius crater with the periodical, systematic acquisition of IR images from permanent stations.

In the first part of the paper we described the experiment design including the technical aspects of the IR camera, the remote control system and the main characteristics of monitored scene. In the second part of the paper we present the analyses performed on a comprehensive time series of 2175 nighttime IR images acquired by the station located at Solfatara in the period October 2004-January 2007 with the double purpose to evaluate the thermal features in the observation period and to determine whether IR information can be useful in the long period monitoring of a volcanically active area. To our knowledge, this is the more comprehensive of such datasets available for a volcanic area.

## **EXPERIMENT DESIGN AND SYSTEM DEVELOPMENT**

The development and the operating assembling of the whole surveillance system have been characterized by a heavy technological integration activity and specific tools development that has not previous noteworthy example to which refers. In fact, the thermal infrared image cameras with uncooled focal plane array measuring systems (microbolometer technology) are of recent availability for the civil market. Such systems find a massive use for process control and quality control in production line and the monitoring of systems in motion or electrical devices; therefore, such monitoring applications implies the use of the thermal cameras as laboratory instruments or just predisposed for indoor installations.

Up to now are not realized any applications for environmental monitoring by permanent stations, still less in extreme conditions as those affecting the volcanic areas; consequently the available thermal imaging cameras are commercialized without the availability of additional tools, like protective housing, data transmission devices or remote control systems.

For this reasons, the integration of the supplementary and necessary technological modules has required the execution of appropriate market surveys to look for special suppliers e\o producers, as well as, the conceiving of specific solutions.

The TIR monitoring network has been conceived in order to satisfy the requirements of continuous long-term volcanological surveillance and has been planned to install the image thermal cameras in two remote sites located on the top of the Vesuvius crater and in the Solfatara crater (Flegrei Fields) respectively (Figure 1).



**Fig. 1.** Location of the Remote Monitoring Stations (RMS). Red dot represents the position of the Surveillance Center.

The whole system consists of two permanent remote monitoring stations, with remote control of the calibration and shooting functionalities of the microbolometric image sensors calibrated on the long thermal infrared wavelengths (Lwave TIR), and a control unit that manages the system by setting the measure session parameters for each single station.

The control unit is located at the surveillance center of the Vesuvius Observatory-INGV in Naples. Its main feature is the management of the remote stations network through a communication system based on two different technological solutions: a master transmission system via GSM frequency network and an emergency system on radio frequency network. The control unit communicates with the RMS's allowing to both configure times and shooting parameters for the image acquisition and run the automatic uploading of the remotely acquired thermal images. In addition, the control unit performs the storage of the transferred thermal images both in its proprietary graphic format for data visualization and, after real-time data conversion, in form of digital ASCII matrix containing the temperature values for further processing.

### **THE TIR REMOTE MONITORING STATION**

The IR cameras used, are the NEC Thermo Tracer TS7302 with uncooled focal plane array measuring systems (microbolometer technology 320x240 pixel) that operates in the spectral range from 8 to 14  $\mu\text{m}$  across a 29° (H) x

22° (V) field of view and a focusing range from 0.5 m to infinity with standard lens.

Up to the beginning of the experiment were not realized any applications for long period outdoor monitoring in extreme conditions as those affecting a volcanic area. For this reason, the first part of the experiment was devoted to integrate the station with protective housing and remote monitoring system (RMS) including data transmission devices. The protective housing, inside of which the camera is placed, has been realized in special stainless steel (Figure 2a) in order to operate in presence of corrosive elements. The shooting window is protected by a germanium glass (Figure 2b) that results transparent to the thermal wavelengths, and is equipped with a mechanical device for covering the germanium glass.

This cover has the dual function to allow the microbolometric sensor calibration and to preserve the integrity and the cleanness of the shooting window during the standby of the thermal camera. The RMS directly manages the phase of the image shots by running in succession the execution of the following actions: (1) turns the thermal camera on, (2) waits for the calibration of the microbolometric sensor, (3) opens the watertight cover, (4) sets the sensibility, the range levels and focus parameters, (5) waits for the image acquisition, (6) closes the watertight cover, (7) uploads the image data acquired by the thermal camera in numerical format through serial RS 232C interface, (8) turns the thermal camera off.

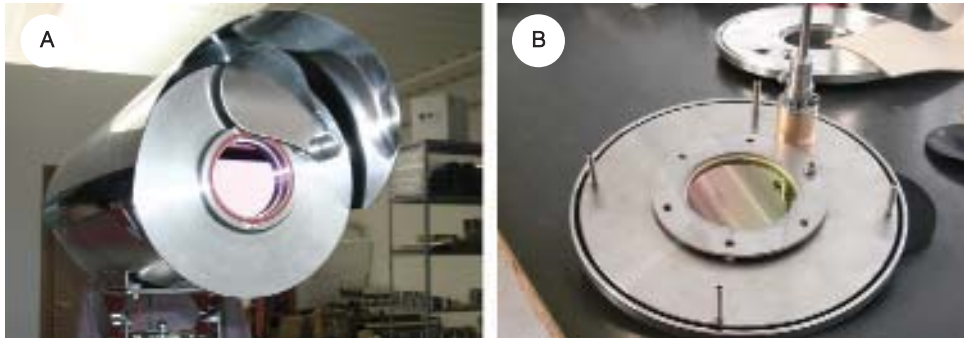


**Fig. 2.** (a) The protective housing realized in special stainless steel. (b) Detail of the frontal flange in which is located the germanium glass.

Following the RMS image storage, the control unit communicates with the RMS and runs the automatic uploading of the remotely acquired thermal images. Table 1 summarizes the time taken by each task from the thermo camera on, up to the image downloading carried out by the control unit.

**Tab. 1.** Time duration of each task involved in the image acquisition and transfer.

Task		Time
Thermo camera	On	00 s
	Check	45 s
	Run	15 s
	Calibration	45 s
Shooting window opening		05 s
Sensibility, range levels and focus set up		10 s
Image acquisition		15 s
Shooting window shutting		05 s
Image transfer from the camera to the RMS		6 m 20 s
Image transfer from the RMS to the Control Unit		3 m 10 s
<b>Total time</b>		<b>11m 50 s</b>

### THE TIR ACQUIRED SCENES

The installation of the remote monitoring stations at Vesuvius crater rim (Figure 3) and at Solfatara (Figure 4) ended at the mid of July 2004 and at the mid of September 2004 respectively. After tests performed on the whole

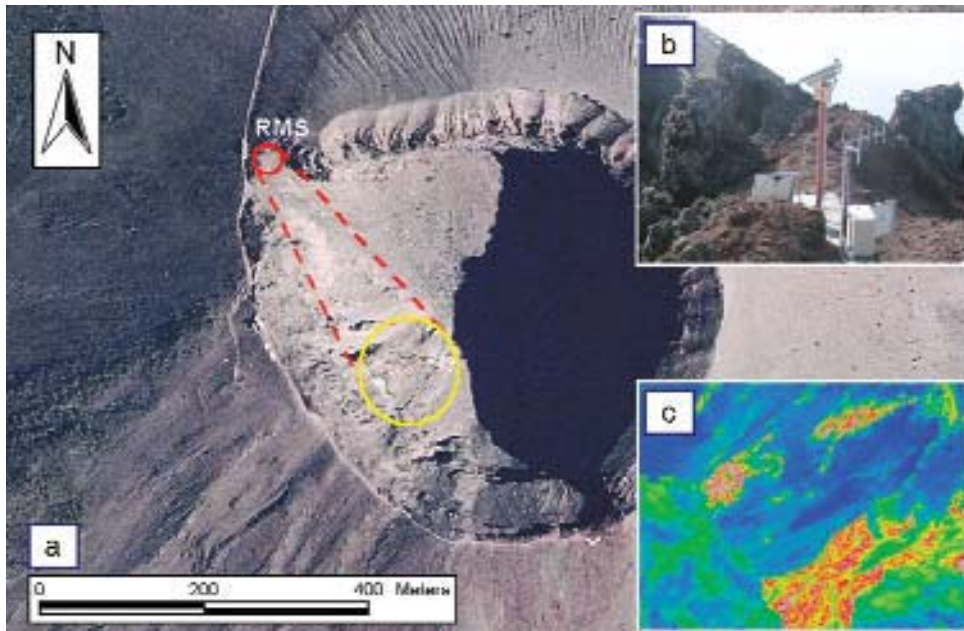


**Fig. 3.** Vesuvius thermal monitoring station. **(a)** viewing geometry, the yellow circle represents the target area; **(b)** the TIR station on the crater rim; **(c)** scene (320x240 pixel) acquired by the remote station in the spectral range of the IR wavelength.

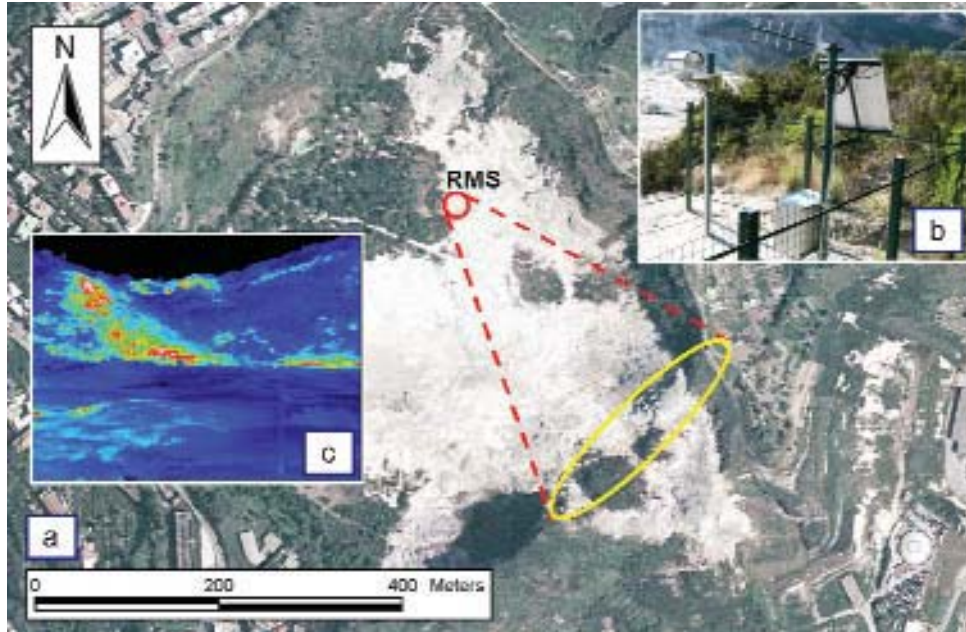


**Fig. 4.** Solfatara thermal monitoring station. **(a)** viewing geometry, the yellow ellipse represents the target area; **(b)** the TIR station in the field; **(c)** scene (320x240 pixel) acquired by the remote station in the spectral range of the IR wavelength.

system began the systematic thermal imaging acquisition. IR images were nighttime collected with the rate of three images per night (acquisition time: Vesuvius 23:00, 01:00, 03:00 UTC and Solfatara 00:00, 02:00, 04:00 UTC). The acquired scene in the spectral IR range are shown in Figure 3c and 4c. For the Vesuvius thermal monitoring station the scene includes part of the SW inner slope of the Vesuvius crater (Figure 3a). This area even if not affected by fumarolic activity shows a significant thermal anomaly depicted by the most radiant pixels in Figure 3c.

For the Solfatara thermal monitoring station the acquired scene includes part of the SE inner slope of the Solfatara crater (Figure 4a) where most radiant pixels correspond to the location of the major fumaroles ( $150^{\circ}\sim 160^{\circ}\text{C}$ ) (Figure 4c), which are sited at the intersection of two active, SW-NE and NW-SE, main faults of Campi Flegrei. This area is the most active sector of the crater. On the basis of previous investigations (Chiodini et al., 2001), can be evaluate that this area releases diffusively  $\sim 15\%$  of the total  $\text{CO}_2$  and heat released by Solfatara crater (i.e.  $\sim 250 \text{ t d}^{-1}$  and  $\sim 13 \text{ MW}$  respectively).

The Solfatara TIR image framing covers a viewing distance that ranges from 40 m up to a maximum of about 500 m, with the main fumaroles field located at an average distance of about 300 m. The Vesuvius TIR image framing

covers a viewing distance that ranges from 100 m up to a maximum of about 400 m, with the main thermal anomalies located at average distances of from about 150 m up to 300m. In both the cases, the increasing viewing distance produces an increase in the pixel size (Table 2) and consequently a decrease in the image resolution.

**Tab. 2.** Pixel size vs. viewing distance.

<b>Distance (m)</b>	10	30	100	300	500
<b>Pixel size (mm)</b>	16	48	160	480	800

The Solfatara TIR imagery was generally of good quality, though it suffers from two minor problems related to the weather conditions: (1) the occasional presence of wide blurred areas due to the condensation of the fumaroles plume and (2) the rare occurrence of heavy rain which caused the homogenization of the IR temperature. On the contrary, the Vesuvius TIR imagery strongly suffers from problems related to the cloudily weather conditions which frequently affect the top of the volcano (the station is located at 1165 m a.s.l.). Moreover, gaps in the GSM transmission often affect the Vesuvius area and this causes the lack of the image transfer to the control unit.

The Vesuvius monitoring station was also affected by two further problems related to: a) the electrostatic charges accumulation that damaged the electronic components of both the RMS and the thermal camera, and b) the failure of the washer impermeability of the protective housing in which the thermal camera is located. In order to restore the functionality of the Vesuvius monitoring station, the broken thermal camera and RMS were replaced and both the line protections and the ground conductor to dissipate the strike into the earth were improved.

Due to the gaps in the image acquisition, related to the operation restoration, the whole TIR image dataset acquired from the Vesuvius remote monitoring station up to 31st may 2007 consists of 1864 images; on the contrary the Solfatara monitoring station, which was not affected by any instrumental problems, acquired 3546 TIR images.

## **THE PORTABLE TIR MONITORING STATION**

Further efforts have been dedicated to design and assemble a portable thermal infrared imagery instrumental system to be employed in temporary surveys in sensitive areas.

The portable station, named TITANO (Thermal Infrared Transportable Apparatus for Nearby Observation), is based on the same technological approach used to operate the permanent monitoring stations with the addition of a tripod necessary to keep up the protective housing containing the thermal camera. The tripod has been conceived and realized adequately solid in order to ensure a stable TIR scene acquisition and it was equipped with telescopic joints to facilitate the clamping on the ground in different field settings. The portable TIR imagery acquisition system was tested during a field survey carried out at Vulcano Island on June 2006 (Figure 5a). On that occasion was estimated in about two hours the time necessary for the installation of the whole acquisition and centralization system, as well as, was verified the right operation of both the GSM and radio transmission systems.

Following the satisfactory results obtained in the first field test, TITANO was used during the Major Emergencies Simulation Exercise (MESIMEX), which, coordinated by the Italian Civil Protection Department, took place from October 18<sup>th</sup> to October 23<sup>rd</sup> 2006 in the Vesuvian area. The exercise, which was focused on the preparedness phase for a major volcanic emergency in the area of Vesuvius, involved several Volcano Expert Teams (VET) which improved the existing monitoring systems with the deployment of added instruments.

Successively, in order to improve the thermal monitoring of the Campi Flegrei, affected by a general small terrain uplift phase started in autumn 2005 (Troise et al., 2007), TITANO station was installed on October 30<sup>th</sup> 2006 and up to now operative, at Pisciarelli (Figure 5b).

This area is located on the outer eastern flank of the Solfatara crater and is characterized by heavy water vapor and CO<sub>2</sub> emissions.

## **ANALYSIS OF THE SOLFATARA TIR IMAGE SERIES**

The reliability of the acquired data was firstly tested with an in situ calibration procedure, performed by comparing IR temperatures with those given by a K type thermocouple.

The experiment consisted in the comparison between IR temperatures and temperatures measured with a K type thermocouple (hereafter named T<sub>ther</sub>). The thermocouple connected with an automatic data logger was installed in an easily identified target (the wood wall of a cabin located in the central sector of the IR scene) whose IR temperature was estimated as the average temperature of 4 pixels, located in the center of the cabin wall (hereafter named T<sub>target</sub>). The experiment started on the 1st August 2006 and ended on the 3<sup>rd</sup> January 2007 producing 434 couples of T<sub>ther</sub> and T<sub>target</sub> values ranging from 273 to 301 K. The temperatures registered by the two independent methods were then compared and, even if the IR measurements resulted systematically lower than T<sub>ther</sub>, the results are very good: the two

*The permanent thermal infrared network for the monitoring of hydrothermal activity at the...*



**Fig. 5. (a)** Field test of TITANO equipment performed on June 2006 at the Vulcano Island. **(b)** From October 30<sup>th</sup> 2006 TITANO is operating at Pisciarelli (Phlegraeen Fields).

temperatures strictly follow the same temporal pattern and show a very high correlation ( $R^2 = 0.989$ ). The positive results allowed us to do not apply any instrumental corrections to the rough data. This choice was based also in the consideration that another source of uncertainty arises from viewing the surface at an oblique angle (Ball and Pinkerton, 2006), an effect which is difficult to be evaluated for every pixel of the image. The availability of a long time series of the same scene, allowed us to analyze the collected thermal imagery in terms of relative temperature variations without apply any correction for the oblique angle view whose possible effects remained unchanged at each location during the monitoring period.

Meteorological data were also specifically acquired during the experiment in order to investigate the dependence of IR data on environmental parameters. IR temperatures are controlled mainly by air temperature which alone explains 92%-97% of the IR temperature variance. This implies a strong seasonal control on the IR temperatures of both background and fumarolized hot areas of Solfatara. In order to remove the effect of ambient temperature variations, which masks the variation caused by endogenous changes, a simple background correction ( $T - T_{\text{target}}$ ) was applied to all the data.

We investigated also the quality of the images (i.e. sharpness, contrast, etc.) which strongly affects the possibility to recognize temperature anomalies and which we found well quantified by the standard deviation (SD) of the IR temperatures of the images. The image quality resulted inversely correlated with the vapor concentration in air. In order to study the evolution in the time of the monitored thermal structure we thus adopted a simple 'quality image' filter based on SD values ( $7.7 < SD < 8.8$ ).

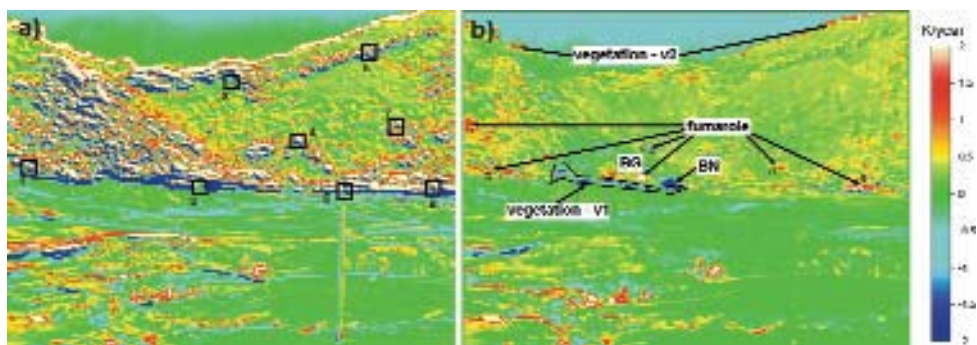


**Fig. 6.** (a) Map of the IR 10-days averaged temperature changes expressed in K/year. A series of contiguous positive and negative anomalies are evident. Eight boxes in the SE inner slope of Solfatara crater are selected to co register the image; (b) Co-registration of the image with the identification of the true temperature changes. Alternations of positive and negative anomalies are disappeared and a few cooling spots (V1 area) and heating spots (areas from a to e and BG area) are highlighted.

On a selected dataset of 2175 TIR images has been performed a pixel by pixel linear regression of  $T-T_{\text{target}}$  with respect to time in order to investigate local temperature changes of the scene. A 10-days average values of  $T-T_{\text{target}}$  at each pixel was considered in order both to reduce the computation time and to smooth high frequency variations. The results are graphically reported in the map of Figure 6a.

The map, which represents the temperature change expressed as K/year, highlights a series of positive and negatives structured anomalies. At any positive anomaly systematically corresponds a negative anomaly, located at left and below of few pixels, suggesting that a movement of the scene occurred during the monitoring period. This unexpected behavior complicates the identification of the real temperature change of the scene. In order to do a co registration of the images, a study of the correlations among selected portions of the scene (boxes from 1 to 8 in Figure 6a) was performed. Practically for each box were determined the shifts in the horizontal and in the vertical axis (DX and DY respectively, expressed as number of pixels) for which the best correlation with respect to a reference case (image n. 1200, 20-02-2006) is obtained. The results in terms of mean values are reported in the DX and DY chronograms of Figures 7a and 7b.

All the boxes are located in the SE inner slope of Solfatara crater in correspondence of hot spots where the contrast with the relatively cold nearby

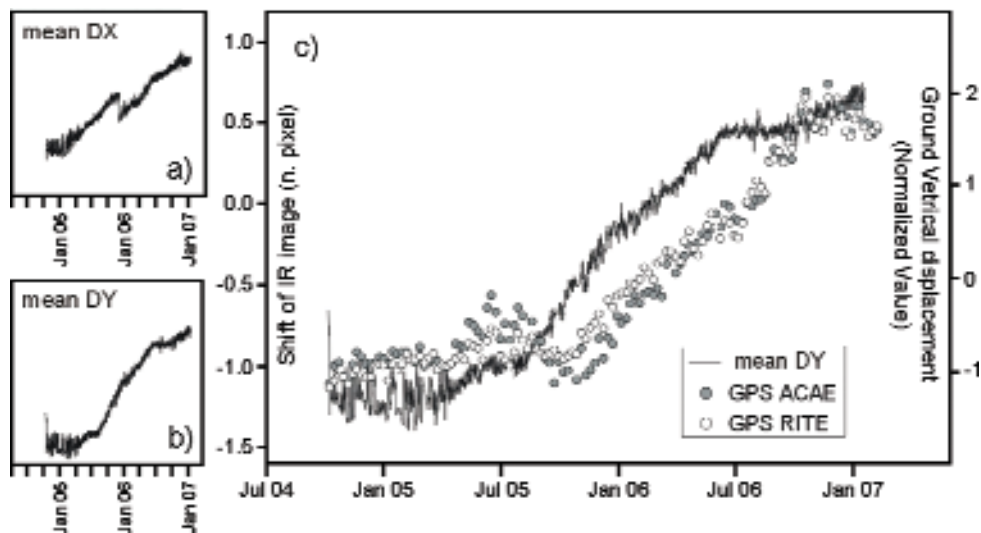


**Fig. 7.** (a) mean horizontal shift (DX) and (b) mean vertical shift (DY) represent the horizontal and the vertical displacement in number of pixels of the whole IR scene with respect to a reference case (image n. 1200, 20-02-2006). (c) Chronogram of the mean vertical displacement of the scene (mean DY) compared to the ground vertical movement recorded by the RITE and ACAE GPS stations (normalized values).

zones makes the computation more efficient and the best results, i.e. where the less noising DX and DY curves were obtained. The results evidenced that all the curves obtained in different portions of the scene show very similar temporal trend. On the base of this similitude it is assumed that the entire IR scene moved both synchronously and at the same velocity following the mean DX and DY vs. time patterns shown in Figures 7a and 7b. This homogeneous behavior of the entire scene suggests that a slow movement affected the camera.

The DY vs time curve shows an intriguing similitude with the ground deformation at CF as returned by GPS continuous monitoring stations located in the neighborhood of the Solfatara (Figure 7c). This observation lead us to suppose that a local deformation of the terrain would have caused the tilt of the pole where the camera is installed and the consequent movement of the scene. We can not exclude that this local deformation is linked to the general terrain uplift phase which occurred at Campi Flegrei in 2005-2006 (Troise et al., 2007).

The best correlation between DY and GPS measurements is obtained by back-shifting ACAE and RITE data of  $\sim 100$  days. This similitude, if confirmed in the next years, would imply that Solfatara is in some way affected by a ground dynamic which anticipates the general deformation at CF. Solfatara would consequently result as an excellent site to study precursors of bradyseismic crisis.

The inferred DY and DX mean values (Figures 7 a and 7b) have been used to perform the co registration of all the images assuming as reference (DX=0, DY=0) the image n. 1200 (acquired on 20-02-2006). Practically for each pixel of each image was computed a new value of T-T\_target as the average of the values of the 4 pixels located in the new position and weighted in function of the surface contribution. Successively, a pixel by pixel regression with respect to time of the corrected T-T\_target data (averaged on a 10 days period) has been performed and the results are graphically shown in Figure 6b.

The map doesn't show any more the structured alternation of positive and negative anomalies which characterizes the analogue picture obtained from the uncorrected values (Figure 6a).

This suggests in general the efficiency of the adopted correction and that Figure 6b can be used to investigate temperature changes occurred at Solfatara during the monitoring period. The main thermal features observed in the map of Figure 6b show that temperature variations affected both the Solfatara crater wall and the areas of the plane nearest to the camera. We focus here our attention to the variations of the Solfatara crater wall being the second ones of smaller dimension and most probably linked to very local processes. The map of Figure 6b suggests that generally the SE inner slope of the Solfatara crater was not affected by important temperature changes, being these generally restricted in the interval from -0.5 K/year to 0.5 K/year. The map however highlights the presence of some spots characterized by higher temperatu-

re increases (red and white colors) and few spots which cooled (blue color). Figure 6b shows that the temperature increase, which is particularly evident at BG site (Bocca Grande: the main fumarole at Solfatara), didn't affect the entire fumarolic field where, contrary, some spots cooled (blue color in Figure 6b). This temperature increase did not regard the maximum temperature of BG fumarole which, in the period of IR monitoring, did not show such large variations remaining at a stationary value of  $161 \pm 2^\circ\text{C}$ . The observed temperature increase regarded the nearby hot soils most probably affected by an increased flux of fumarolic fluids. It is worth noting that also steam velocity of BG fumarole, a parameter monitored since spring 2005, shows an increase in the flux of the fumarolic fluids, suggesting that the IR temperature anomaly detected in the observation period is caused by the increased fumarolic flux. On the contrary, the temperature decreases are not linked to the variation of the hydrothermal source rather they reflect anthropic jobs or vegetation growth. In particular the BN (Bocca Nuova) site, another high temperature fumarole ( $\sim 150^\circ\text{C}$ ) shows a marked cooling. In this case the temperature variation registered by the automatic station was caused by the building in October-November 2006 of a tourist pathway that goes around the BN fumarole. The work caused a clear decrease of the temperature of the area, variation not linked to the activity of the volcano. Other temperature decreases were observed in the area labeled 'vegetation-v1' in Figure 6b. In this case the temperature decrease reflects the fact that the relatively hot pixels of the Solfatara crater wall were progressively occupied by the colder vegetation growing in the spring season. The same process explains also the positive anomalies at the border between the sky and the ground ('vegetation-v2' in Figure 6b), being in this case the relatively cold pixels of the sky progressively occupied by the hotter vegetation.

## CONCLUSIONS

The set up of Infrared (IR) automatic stations for the continuous long-term monitoring of the shallow thermal structure of hydrothermal zones was the main objective of this research. With respect to previous IR applications, most of which regarded the study of relatively quick processes associated to volcanic eruptions, our experiment was finalized to detect and quantify over long periods slow temperature changes of shallow thermal structures of quiescent volcanoes. In particular our experiment was designed to monitor a significant portion of the Solfatara fumarolic field and of the Vesuvius crater with the periodical, systematic acquisition of IR images from a permanent station. The analysis of two years of IR images acquired at the Solfatara gives a reliable picture, rich in particulars, of the temperature changes and important indications on the origin of the changes. The analysis of the data showed the occurrence of various processes, which were proved on the basis of inde-

pendent observations, such as anthropic jobs, vegetation growth and relatively low flux increases of hydrothermal fluids. It is note worth that these signs were detected in a system characterized at the present moment by a level of activity relatively low with respect to those systems affected by real volcanic crisis where more spectacular results will be expected.

An important point is that the images can be suitably filtered from ambient effects using simple corrections based on data belonging at the image itself. This makes the system independent from the availability of other data. Our filtering was based in fact on a background temperature defined in the scene, on the standard deviation of each image and on a procedure based on image data for the co-registration. These features make the system almost autonomous and able to work also in remote and impervious sites resulting as a suitable tool for volcanic surveillance.

#### **ACKNOWLEDGMENTS**

We thank Prospero De Martino and Umberto Tamaro for the GPS data. This work was partially funded by the 2000-2006 National Operating Program and by the Italian Dipartimento della Protezione Civile in the frame of the 2004-2006 agreement with Istituto Nazionale di Geofisica e Vulcanologia.

#### **REFERENCES**

- Ball, M., and H. Pinkerton (2006), Factors affecting the accuracy of thermal imaging cameras in volcanology, *J. Geophys. Res.*, 111, B11203.doi:10.1029/2005JB003829.
- Calvari, S., and H. Pinkerton (2004), Birth, growth and morphologic evolution of the 'Laghetto' cinder cone during the 2001 Etna eruption, *J. Volcanol. Geotherm. Res.*, 132, 225-239.
- Calvari, S., L. Spampinato, L. Lodato, A. J. L. Harris, M. R. Patrick, J. Dehn, M. R. Burton, and D. Andronico (2005), Chronology and complex volcanic processes during the 2002-2003 flank eruption at Stromboli volcano (Italy) reconstructed from direct observations and surveys with a handheld thermal camera, *J. Geophys. Res.*, 110, B02201.doi:10.1029/2004JB003129.
- Chiodini, G., F. Frondini, C. Cardellini, D. Granieri, L. Marini, and G. Ventura (2001), CO<sub>2</sub> degassing and energy release at Solfatara Volcano, Campi Flegrei, Italy, *J. Geophys. Res.*, 106, 16,213-216,221.
- Harris, A. J. L., J. Dehn, M. R. Patrick, S. Calvari, M. Ripepe, and L. Lodato (2005), Lava effusion rates from hand-held thermal infrared imagery: an example from the June 2003 effusive activity at Stromboli, *Bull. Volcanol.*, 68, 107-117.
- Johnson, J. B., A. J. L. Harris, and R. P. Hoblitt (2005), Thermal observations of gas pistonning at Kilauea Volcano, *J. Geophys. Res.*, 110, B11201.doi:10.1029/2005JB003944.
- Kaneko, T., and M. J. Wooster (1999), Landsat infrared analysis of fumarole activity at Unzen Volcano: time-series comparison with gas and magma fluxes, *J. Volcanol. Geotherm. Res.*, 89, 57-64.

- Lautze, N. C., A. J. L. Harris, J. E. Bailey, M. Ripepe, S. Calvari, J. Dehn, S. K. Rowland, and K. Evans-Jones (2004), Pulsed lava effusion at Mount Etna during 2001, *J. Volcanol. Geotherm. Res.*, 137, 231- 246.
- Lodato, L., L. Spampinato, A. J. L. Harris, S. Calvari, J. Dehn, and M. Patrick (2006), The morphology and evolution of the Stromboli 2002-2003 lava flow field: an example of a basaltic flow field emplaced on a steep slope., *Bull. Volcanol.*doi: 10.1007/s00445-006-0101-6.
- Oppenheimer, C., P. W. Francis, D. A. Rothery, R. W. T. Carlton, and L. S. Glaze (1993), Infrared image analysis of volcanic thermal features; Lascar Volcano, Chile, 1984-1992, *J. Geophys. Res.*, 98, 4269-4286.
- Pinkerton, H., M. James, and A. Jones (2002), Surface temperature measurements of active lava flows on Kilauea volcano, Hawai'i, *J. Volcanol. Geotherm. Res.*, 113, 159-176.
- Troise, C., G. De Natale, F. Pingue, F. Obrizzo, P. De Martino, U. Tammaro, and E. Boschi (2007), Renewed ground uplift at Campi Flegrei caldera (Italy): New insight on magmatic processes and forecast., *Geophys. Res. Lett.*, 34, L03301.doi:10.1029/2006GL028545.
- Vaughan, R. G., S. J. Hook, M. S. Ramsey, V. J. Realmuto, and D. J. Schneider (2005), Monitoring eruptive activity at Mount St. Helens with TIR image data, *Geophys. Res. Lett.*, 32, L19305.doi:10.1029/2005GL024112.

Finito di stampare nel mese di aprile 2008  
presso Officine Grafiche Francesco Giannini & Figli S.p.A. – Napoli